Nanoscale "Dark State" Optical Potentials for Cold Atoms

M. Łącki,[1,2] M. A. Baranov,[1,2] H. Pichler,[1,2,3,4] and P. Zoller[1,2]
[1]Institute for Quantum Optics and Quantum Information of the Austrian Academy of Sciences, A-6020 Innsbruck, Austria
[2]Institute for Theoretical Physics, University of Innsbruck, A-6020 Innsbruck, Austria
[3]ITAMP, Harvard-Smithsonian Center for Astrophysics, 60 Garden Street, Cambridge, Massachusetts 02138, USA
[4]Physics Department, Harvard University, 17 Oxford Street, Cambridge, Massachusetts 02138, USA
(Received 26 July 2016; published 30 November 2016)

We discuss the generation of subwavelength optical barriers on the scale of tens of nanometers, as conservative optical potentials for cold atoms. These arise from nonadiabatic corrections to Born-Oppenheimer potentials from dressed "dark states" in atomic Λ configurations. We illustrate the concepts with a double layer potential for atoms obtained from inserting an optical subwavelength barrier into a well generated by an off-resonant optical lattice, and discuss bound states of pairs of atoms interacting via magnetic dipolar interactions. The subwavelength optical barriers represent an optical "Kronig-Penney" potential. We present a detailed study of the band structure in optical Kronig-Penney potentials, including decoherence from spontaneous emission and atom loss to open "bright" channels.

DOI: 10.1103/PhysRevLett.117.233001

Optical potentials generated by laser light are a fundamental tool to manipulate the motion of cold atoms with both conservative and dissipative forces [1,2]. Paradigmatic examples of conservative optical potentials are optical dipole traps from a focused far off-resonant light beam, or optical lattices (OLs) generated by an off-resonant standing laser wave, as the basis of the ongoing experimental effort to realize atomic Hubbard models [3]. The underlying physical mechanism is the second-order ac Stark shift of an electronic atomic level, which is proportional to the light intensity. Optical potential landscapes, which can be designed, will thus reflect and be limited by the achievable spatial variation of the light intensity. For light in the far field, i.e., for optical trapping far away from surfaces (compare Refs. [4–8]), this spatial resolution will thus be given essentially by the wavelength of the light λ. In the quest to realize free-space optical subwavelength structures for atoms [9–15] we will describe and study below a family of conservative optical potentials, which arise as nonadiabatic corrections to dark states (DSs) in atomic Λ-type configurations [16,17], building on the strong nonlinear atomic response to the driving lasers. The present scheme should allow the realization of *optical barriers* for atoms on the scale of tens of nanometers, and in combination with traditional optical potentials and lattices the formation of a complex "nanoscale" optical landscape for atoms. Our discussion should be of particular interest for realizing many-atom quantum dynamics as a strongly interacting many-body systems, where atomic energy scales and interactions, such as magnetic dipolar couplings [18–22], are strongly enhanced by subwavelength distances.

To illustrate the nanoscale optical potentials we can construct, we show in Fig. 1 a setup where a subwavelength barrier of width ℓ is inserted into a potential well. This potential well can be created, for example, with a (standard) off-resonant OL $V_L(x) = V_0 \sin^2(k_L x) \approx V_0 (k_L x)^2$ with $\lambda_L \equiv 2\pi/k_L$ the wavelength of the trapping laser, and we denote its ground state size by a_L. Thus, our aim is to create a double well potential for atoms on the subwavelength scale $\ell \ll a_L \ll \lambda_L/2$. By adjusting the height, and by displacing the subwavelength barrier we can control the tunnel coupling between the wells, strongly enhanced relative to the standard OL with lattice period $\lambda_L/2$. In a 3D (2D) setup this realizes a double layer (wire), with subwavelength separation. Loading magnetic atoms or polar molecules with dipolar interactions into these structures, we benefit from the strongly enhanced energy scales for interlayer (wire) interactions.

We propose and analyze below the physical realization of such a setup, and we will mainly focus on a 1D model considering atomic motion along x. The subwavelength barrier is obtained by choosing an atomic Λ transition with two long-lived ground (spin) states $|g_1\rangle \equiv |\downarrow\rangle$, $|g_2\rangle \equiv |\uparrow\rangle$ [Fig. 1(b)] [23,24], which are coupled by a Raman transition. The first leg of the Raman coupling is a strong control laser with Rabi frequency $\Omega_c(x) = \Omega_c \sin(kx)$ as a standing wave with wavelength $\lambda = 2\pi/k$ along x, and the second is a weak probe laser with Rabi frequency Ω_p with propagation direction perpendicular to the axis x [25]. We denote the ratio of Rabi frequencies as $\epsilon \equiv \Omega_p/\Omega_c \ll 1$. The lasers are tuned to satisfy the Raman resonance condition, while the detuning Δ from the excited state $|e\rangle$ can be near or off resonant. The relevant Hamiltonian is $H = -\hbar^2 \partial_x^2/2m + H_a(x)$ [23], as a sum of the kinetic energy and the internal atomic Hamiltonian

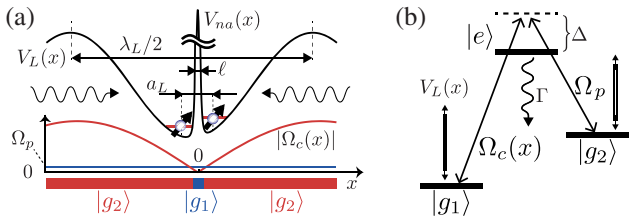

FIG. 1. (a) A double well potential for atoms is created by inserting an optical subwavelength barrier $V_{na}(x)$ with width ℓ into a potential well generated with an off-resonant OL $V_L(x)$ with lattice period $\lambda_L/2$, and size of the vibrational ground state a_L, such that $\ell \ll a_L \ll \lambda_L/2$. The subwavelength barrier is obtained with an atomic Λ-system supporting a "dark state" as superposition of the two atomic ground states $|g_1\rangle$ and $|g_2\rangle$ (b), where a resonant Raman coupling from a strong control field $\Omega_c(x) = \Omega_c \sin(kx)$ $(k = 2\pi/\lambda)$ and a weak probe field Ω_p connects the two ground states (see text).

$$H_a = \hbar\left[\left(-\Delta - i\frac{\Gamma}{2}\right)|e\rangle\langle e| + \frac{\Omega_c(x)}{2}|e\rangle \times \langle g_1| + \frac{\Omega_p}{2}|e\rangle\langle g_2| g_2 + \text{H.c.}\right]$$

written in a rotating frame, and with Γ the spontaneous decay rate of $|e\rangle$. We can add to the above Hamiltonian a trapping potential for the ground states $V(x)$ to generate the well of Fig. 1. This is realized, e.g., as a 1D off-resonant lattice $V_L(x) = V_0 \sin^2(k_L x)$ with an effective $k_L = 2\pi/\lambda_L$, i.e., $V(x) \equiv V_L(x)\sum_{i=1,2}|g_i\rangle\langle g_i|$. This far off-resonant OL potential acts equally on both ground states, and thus preserves the resonance Raman condition independent of x.

We are interested in the regime of slow atomic motion, where the kinetic energy [and trapping potential $V(x)$] are small relative to the energy scales set by H_a. In the spirit of the Born-Oppenheimer (BO) approximation [26–29] we diagonalize $H_a(x)|E_\sigma(x)\rangle = E_\sigma(x)|E_\sigma(x)\rangle$ $(\sigma = 0, \pm)$ to obtain position dependent dressed energies,

$$E_0(x) = 0, E_\pm(x) = \frac{\hbar}{2}\left[-\tilde{\Delta} \pm \sqrt{\Omega_p^2 + \Omega_c^2(x) + \tilde{\Delta}^2}\right],$$

with $\tilde{\Delta} \equiv \Delta + i(\Gamma/2)$, playing the role of adiabatic BO potentials for the atomic motion. Such a Λ configuration supports an atomic DS $E_0 = 0$ as a linear combination of the ground states, $|E_0(x)\rangle = -\cos\alpha(x)|g_1\rangle + \sin\alpha(x)|g_2\rangle$ with $\alpha(x) = \arctan[\Omega_c(x)/\Omega_p]$, which for an atom at a given position x (at rest) is decoupled from the exciting Raman beams. The identity of this DS changes in space on a subwavelength scale [10,24]: in regions $|\Omega_c(x)| \gg \Omega_p$ we have $|E_0\rangle \sim |g_2\rangle$, while $|\Omega_c(x)| \ll \Omega_p$ defines a region $\ell \equiv \epsilon\lambda/2\pi \ll \lambda$ with $|E_0\rangle \sim |g_1\rangle$ and thus a spatial subwavelength spin structure [bottom of Fig. 1(a)].

An atom prepared in the DS, and moving slowly in space will, in accordance with an adiabaticity requirement [30], remain in this DS, and the internal state will change its internal spin identity according to $|E_0(x)\rangle$ on the scale $\ell \ll \lambda$. Correspondingly, there will be nonadiabatic corrections to this motion. As shown below, these nonadiabatic corrections take on the form of a subwavelength optical barrier representing a conservative potential

$$V_{na}(x) = \frac{\hbar^2}{2m}(\partial_x\alpha)^2 \equiv E_R\frac{\epsilon^2\cos^2(kx)}{[\epsilon^2 + \sin^2(kx)]^2}, \qquad (1)$$

with $E_R = \hbar^2k^2/2m$ the recoil energy and atomic mass m. The effective 1D Hamiltonian for the atomic motion is thus $h = -\hbar^2\partial_x^2/2m + V_L(x) + V_{na}(x)$. In Fig. 1(a) this realizes the subwavelength barrier, where the vibrational ground state of the OL potential $V_L(x)$ of size a_L is split into a double well for $\ell \ll a_L$. We note that $V_{na}(x)$, apart from the overall scale E_R, depends only on $\epsilon = \Omega_p/\Omega_c$. For $\epsilon \ll 1$, $V_{na}(x)$ is a sequence of potential hills with spacing $\lambda/2$, width $\ell \equiv \epsilon\lambda/2\pi \ll \lambda/2$, and height $E_R/\epsilon^2 \gg E_R$ [cf. Fig. 2(b)], and has for $\epsilon \ll 1$ a form reminiscent of a repulsive Kronig-Penney δ-like comb $V_{na}(x) \to \sum_n E_R\lambda/(4\epsilon)\delta(x - n\lambda/2)$ [31]. For Raman beams derived from the same laser source this potential is insensitive to both intensity and phase fluctuations. We emphasize that the mechanism behind Eq. (1) is related to nonadiabatic corrections, as described by Olshanii and Dum [27], and is conceptually different from schemes relying on a substructuring ac Stark based OLs by radio frequency or laser fields [9,11], or in combination with DSs [10]. Figure 2(a) is a plot of the BO potentials $E_{0,\pm}(x)$ for blue detuning

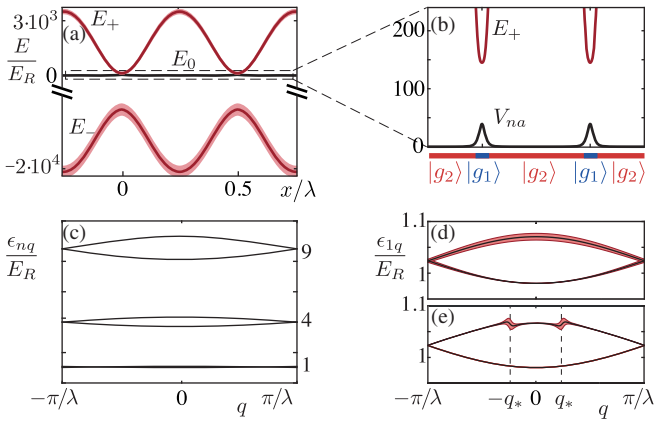

FIG. 2. (a) BO potentials $E_0(x) = 0$ (black line) and $E_\pm(x)$ [red line, with line width indicating $\text{Im}E_\pm(x)$] for DS and BS, respectively. Parameters: $\Omega_c = \Delta = 1.7 \times 10^4 E_R$, $\epsilon = 0.16$, $\Gamma = 5 \times 10^2 E_R$. (b) Zoom showing $V_{na}(x)$ (black) and the lower part of $E_+(x)$ (red). (c) Lowest Bloch bands $\epsilon_{n,q}$ for $V_{na}(x)$ for Brillouin zone $|q| < \pi/\lambda$ (see text); $\epsilon = 0.1$. (d),(e) Zooms of the lowest Bloch band of the DS lattice, including couplings to BSs for $\epsilon = 0.1$, $\Omega_p = 2 \times 10^3 E_R$, $\Gamma = 10^3 E_R$ (d), and $\Gamma = 10E_R$ (e) (see text and Ref. [32]). Black lines indicate $\text{Re}\epsilon_{1,q}$, and red shadings the widths $\text{Im}\epsilon_{1,q} = -\hbar\gamma_{1,q}/2$.

$\Omega = \Delta > 0$ and $\epsilon = 0.16$ with parameters chosen to illustrate the main features (with similar results for red detuning). For $\Delta \gg \Omega_{c,p}$, the bright state (BS) $|E_+(x)\rangle \to \sin\alpha(x)|g_1\rangle + \cos\alpha(x)|g_2\rangle$ corresponds to the standard OL $E_+(x) \to (\hbar/4)[\Omega_p^2 + \Omega_c^2(x)]/[\Delta + (i/2)\Gamma]$ as a second order Stark shift [cf. Fig. 2(a)].

To quantify the above discussion and assess the validity of the BO approximation we present now a derivation and analysis of optical potentials arising from nonadiabatic corrections to atomic motion, and effects of spontaneous emission (due to admixture of bright channels). Expanding the atomic wave function in the BO channels, $|\Psi(x)\rangle = \sum_\sigma \Psi_\sigma(x)|E_\sigma(x)\rangle$, results in the coupled channel equation for $\Psi_\sigma(x)$ [27,29]. The corresponding Hamiltonian is $\mathcal{H} = [-i\hbar\partial_x - A(x)]^2/2m + V(x)$, where the diagonal matrix $V_{\mu\sigma}(x) = E_\sigma(x)\delta_{\mu\sigma}$ contains BO potentials (see Fig. 2). Nonadiabatic processes, coupling the BO channels, arise from the spatial variation of the internal eigenstates, $-i\hbar\partial_x|E_\sigma(x)\rangle = \sum_\mu |E_\mu(x)\rangle A_{\mu\sigma}(x)$ with scaling $A_{\mu,\sigma} \sim \hbar/\ell$ (see Ref. [32]).

We are interested in the regime of approximate adiabatic decoupling of BO channels. This requires that the separations between DS and BS are larger than the channel couplings. For the DS, the lowest order contribution from the A^2 term gives rise to the nonadiabatic (conservative) potential (1) [see Fig. 2(b)], with consistency requirement $V_{na}(x) \ll \min|E_\pm(x)|$. We discuss this by setting the external potential $V(x) = V_L(x) = 0$, and studying the 1D band structure for the Λ scheme of Fig. 1(b). We compare below the results for (i) the single-channel DS potential $V_{na}(x)$ with (ii) the exact diagonalization of the (non-Hermitian) Hamiltonian H, using a Bloch ansatz $\Psi(x) = e^{iqx}u_{n,q}(x)$ with quasimomentum q to obtain the (complex) energies $\epsilon_{n,q}$. In the first case we have a unit cell $\lambda/2$ and thus a Brillouin zone $|q| < 2\pi/\lambda$, while H has periodicity λ, and, thus, $|q| < \pi/\lambda$, so that the bands of the first case appear as "folded back" in the second case [see Figs. 2(c), 2(d), 2(e)].

For the DS potential $V_{na}(x)$ the band structure is for $\epsilon \ll 1$ analogous to that of a Kronig-Penney model [31]. For the lowest Bloch bands $n = 1, 2, \ldots$ in the DS channel 0 we obtain (see Ref. [32])

$$\epsilon_{n,q}^{(0)} \approx E_R n^2 \left\{1 + \frac{4\epsilon}{\pi^2}\left[1 + (-1)^n \cos\frac{\pi q}{k}\right]\right\}, \qquad |q| \le \frac{2\pi}{\lambda} \tag{2}$$

in very good quantitative agreement with the band structure obtained from H. These bands have narrow width $\sim\epsilon$, corresponding to a hopping amplitude $J_n = 2E_R\epsilon n^2/\pi^2$ in the terminology of the tight-binding Hubbard model [3]. The energy offset of these bands $E_R n^2$ is close to the levels in the infinitely deep rectangular well of the width $\lambda/2$, with anharmonic band spacing (independent of ϵ, and thus the height of the potential). The Wannier functions associated with these bands resemble the eigenfunctions of a box potential. This is in marked contrast to the band structure in a $V(x) = V_0\sin^2(kx)$ OL, where energies of low lying bands are harmonic oscillatorlike, and the Wannier functions are strongly localized $a_L \ll \lambda/2$ (Lamb-Dicke regime) [3]. The spectroscopy of these bands could be investigated with time of flight, and by modulating the lattice. A discussion of this and of loading the lowest Bloch band can be found in Ref. [32].

For the DS channel 0, the nonadiabatic couplings to the bright (dissipative) BO channels $\pm$ result in a small correction $\delta\epsilon_{n,q}$ to the dispersion, which contains a imaginary part $\mathrm{Im}\delta\epsilon_{n,q} = -\hbar\gamma_{n,q}/2 < 0$, signaling decay of atoms in the Bloch band. Figures 2(d) and 2(e) indicate the width of the lowest Bloch band $\gamma_{1,q}$, by a red-shaded region around the dispersion relation $\epsilon_{1,q}$, as obtained from a numerical solution of the coupled channel equations. The parameters are chosen to illustrate the limits of a "large" and "small" decay width Γ (see Ref. [32]). We note that in both cases $\gamma_{1,q} \ll J_1$; i.e., dissipative corrections are typically very small, while $\gamma_{1,q}$ shows a nontrivial q dependence. In Fig. 2(d) we can parametrize

$$\gamma_{1,q} \approx \gamma_1 \sin^2(\pi q/2k), \qquad |q| \le \frac{2\pi}{\lambda} \tag{3}$$

(see Ref. [32]), where for the lowest Bloch band the decay increases with q [Fig. 2(d)]—something we expect from a STIRAP scenario [17], where faster atomic motion leads to a stronger violation of adiabaticity and thus depopulation of the DS. In contrast, Fig. 2(e) shows the appearance of *resonances* in q: as discussed in Ref. [32] these appear when for a given $q = q_\star$ the energies in the dark channel 0 becomes energetically degenerate with energies in the bright open channel $-$, $\epsilon_{n,q_\star}^{(0)} \approx \mathrm{Re}\epsilon_{n,q_\star+k}^{(-)}$. With increasing Γ relative to the strength of the nonadiabatic couplings these resonances get successively washed out, transitioning to the generic behavior of Fig. 2(d). We refer to Ref. [32] for a detailed discussion of $\gamma_{n,q}$, and, in particular, scaling with system parameters.

Returning to Fig. 1(a) we point out that the above discussion can be generalized to DSs in 2D and 3D configurations. Thus, we can replace $\Omega_c(x) \to \Omega_c(x, y)$ and $V_L(x) \to V_L(x, y)$, while preserving the existence of a DS $|E_0(x, y)\rangle$, allowing us to add a (standard) OL for motion in the y direction, or the realization of an atomic double wire with separation ℓ.

We now turn to a study of quantum many-body physics, and discuss as an illustrative example the motion of two atoms confined in the subwavelength structure of Fig. 1, and interacting via magnetic dipolar interactions. The validity of (1) in a many-body Schrödinger equation will be discussed below. We assume that the two-body physics can be modeled by the external motion of each

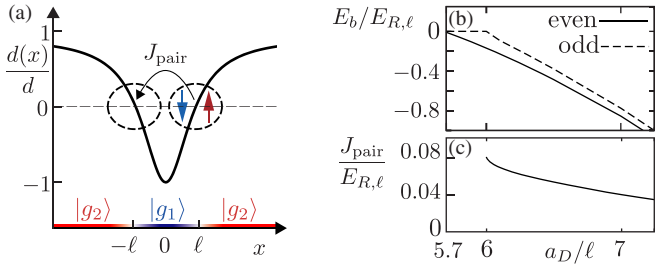

FIG. 3. (a) Position-dependent dipole moment $d(x)/d$, for $-d_1 = d_2 = d$. Molecules exist as bound states of two atoms due to dipolar attraction at the interfaces, where $d(x)$ changes sign. (b) Bound state energies E_b, and (c) hopping amplitude J_{pair} of molecules between the two interfaces for $\epsilon = 0.1$ in units of $E_{R,\ell} \equiv \hbar^2/2m\ell^2 = E_R/\epsilon^2$.

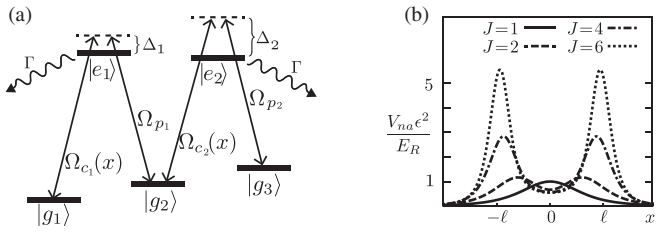

FIG. 4. (a) Atomic zigzag (double-Λ) configuration with $\Omega_{c_i}(x)$ strong standing waves and Ω_{p_i} weak probe beams, and (b) the corresponding nonadiabatic optical potentials on the subwavelength scale $\ell \ll \lambda$ for an atomic angular momentum $J_g = J_e \equiv J$ transition, where the Zeeman levels are coupled by circularly polarized laser fields. With increasing J a double barrier structure develops.

atom governed by $V_L(x) + V_{na}(x)$, while the internal state is the BO channel $|E_0(x)\rangle$, with the unique feature of an x-dependent internal state [see bottom of Fig. 1(a)]. We consider two ground states (spins) with associated magnetic dipole moments d_1, d_2, oriented according to a quantization axis defined by an external magnetic field, so that each atom acquires an effective position-dependent dipole moment, $d(x) = d_1\cos^2\alpha(x) + d_2\sin^2\alpha(x)$. Figure 3(a) is a plot of this dipole moment for a choice of states with $-d_1 = d_2 \equiv d$, with the spatial variation of $|E_0(x)\rangle$ now imprinted as a variation of $d(x)$ on the scale ℓ. The magnetic (dipolar) interactions between the atoms is thus modulated by this spatial dependence. There are two generic situations, the first (i) with the dipole moments oriented along x, and the second (ii) with dipole oriented perpendicular. In the first case, two atoms on opposite sides of the barrier in the double layer attract each other in a head-to-tail configuration. For the case of electric dipole moments as realized with polar molecules, stored in a 2D double layer from an OL with $\lambda/2$ separation, the formation of bound states as building blocks for quantum phases has been studied [46–49]. Here we note that this physics of strong interactions becomes accessible when the dipolar length $a_D = md^2/\hbar^2$ [18,19], characterizing the dipolar interactions [50], is comparable to the average distance between the atoms (here $\sim a_L$ with $\ell \ll a_L \ll \lambda_L$).

Instead, we focus here on physics of perpendicular dipole moments (ii) at the *interface* between the spin structure, $|g_1\rangle \leftrightarrow |g_2\rangle$, as shown in Fig. 3. If the dipoles are oriented perpendicular to x, atoms on opposite sites of the interface attract each other, thus allowing for the formation of a bound state as a "domain wall" molecule. The situation is illustrated by the following two-particle Hamiltonian (see Ref. [32] for detailed description):

$$H = \sum_{i=1,2}\left[-\frac{\hbar^2\partial_{x_i}^2}{2m} + V_{na}(x_i)\right] + \frac{d(x_1)d(x_2)}{|x_1 - x_2|^3}, \quad (4)$$

with $d(x)$ modulated on the scale ℓ, assuming strong confinement $\ell_\perp < \ell$ in the transverse plane (and setting $V_L = 0$). According to Fig. 3 we find that the requirement for a bound state of size ℓ to form is $a_D/\ell \sim 6$ [51–53], where the domain wall molecules sit on the slope of the nonadiabatic potential. These molecules exist at both the left and right interfaces $\pm\ell$, and can hop between them, realizing a double layer with subwavelength distance. The (potentially large) amplitude J_{pair} for hopping is reflected as a hybridization of molecular orbitals on the left and right interfaces, seen in Fig. 3 as a splitting between the even and odd states. We can also obtain *trimers* as bound states of three atoms, where two spin-up dipoles sit to the left (right) of $-\ell$ ($+\ell$) and a spin-down in the middle.

From an atomic physics point of view, a Λ scheme and a nonadiabatic DS potential can be realized with both alkali and alkaline earth atoms, where two ground states are chosen from a Zeeman or hyperfine manifold. Remarkably, these nonadiabatic potentials exist, on the level of single-atom physics, as *conservative* optical potentials even *on resonance* ($\Delta = 0$) and for short lived excited states (but still $\Omega_{c,p} \gg \Gamma$). In going off resonance, the nonadiabatic conservative potential will persist albeit with an increasing requirement for laser power to satisfy the adiabaticity requirement, in particular $V_{na}(0) < (\hbar/4)\Omega_p^2/\Delta$ ($\Omega_p \ll \Delta$) for $\Delta > 0$ as shown in Figs. 2(a) and 2(b). With increasing detuning, the three-level model will eventually break down, and the coupling to several excited states may become important. This situation parallels the challenges in realizing spin-dependent OLs [54–57], and spin-orbit coupling in Λ systems with Alkali atoms [58–65], where the electronic spin-flip implicit in coupling two ground states via Raman transition is suppressed for detunings larger than the fine structure splitting of the excited state. We note, however, the encouraging prospects provided by lanthanides in realizing spin-orbit couplings [19,66,67] and synthetic gauge fields [68,69]. In a many-atom context, going to off-resonant laser excitation is a necessary requirement to suppress inelastic collision channels (involving laser excitation at the Condon point), and we expect a similar requirement here. As discussed in the context of

polar molecules, long range repulsive dipolar interactions in combination with low-dimensional trapping (1D or 2D) can provide a shield in atom-atom collisions at low energies [70], thus suppressing inelastic loss and instabilities from short range physics [71].

To conclude, Λ-type configurations with nonadiabatic DS optical potentials are readily generalized to zigzag configurations as in Fig. 4(a) (see also Ref. [32]). This yields a *double-peaked structure* on the scale ℓ as in Fig. 4(b). These ideas enable writing complex spatial spin patterns [10] and associated landscapes of nonadiabatic potentials. On the many-atom level spatially varying internal structures result in *position-dependent* interparticle interactions. This provides a novel setting for many-body atomic systems, illustrated here for magnetic dipole-dipole interactions, and poses interesting questions as quantum chemistry in atomic collisions at subwavelength distances.

We thank J. Budich, L. Chomaz, J. Dalibard, M. Dalmonte, F. Ferlaino, R. Grimm, T. Pfau, and T. Porto for helpful comments. Work at Innsbruck is supported by the ERC Synergy Grant UQUAM, the Austrian Science Fund through SFB FOQUS (FWF Project No. F4016-N23), and EU FET Proactive Initiative SIQS. H. P. was supported by the NSF through a grant for the Institute for Theoretical Atomic, Molecular, and Optical Physics at Harvard University and the Smithsonian Astrophysical Observatory.

Note added.—Recently we have become aware of Ref. [72] by Jendrzejewski *et al.*, which overlaps with the first part of our Letter.

[1] D. Guéry-Odelin and C. Cohen-Tannoudji, *Advances in Atomic Physics* (World Scientific, Singapore, 2011).
[2] M. Lewenstein, A. Sanpera, and V. Ahufinger, *Ultracold Atoms in Optical Lattices: Simulating Quantum Many-Body Systems* (Oxford Univ. Press, Oxford, 2012).
[3] I. Bloch, J. Dalibard, and W. Zwerger, Rev. Mod. Phys. **80**, 885 (2008).
[4] R. Mitsch, C. Sayrin, B. Albrecht, P. Schneeweiss, and A. Rauschenbeutel, Nat. Commun. **5**, 5713 (2014).
[5] J. Thompson, T. Tiecke, N. de Leon, J. Feist, A. Akimov, M. Gullans, A. Zibrov, V. Vuletić, and M. Lukin, Science **340**, 1202 (2013).
[6] A. González-Tudela, C.-L. Hung, D. E. Chang, J. I. Cirac, and H. Kimble, Nat. Photonics **9**, 320 (2015).
[7] D. E. Chang, J. D. Thompson, H. Park, V. Vuletić, A. S. Zibrov, P. Zoller, and M. D. Lukin, Phys. Rev. Lett. **103**, 123004 (2009).
[8] M. Gullans, T. G. Tiecke, D. E. Chang, J. Feist, J. D. Thompson, J. I. Cirac, P. Zoller, and M. D. Lukin, Phys. Rev. Lett. **109**, 235309 (2012).
[9] W. Yi, A. Daley, G. Pupillo, and P. Zoller, New J. Phys. **10**, 073015 (2008).
[10] M. Kiffner, J. Evers, and M. S. Zubairy, Phys. Rev. Lett. **100**, 073602 (2008).
[11] S. Nascimbene, N. Goldman, N. R. Cooper, and J. Dalibard, Phys. Rev. Lett. **115**, 140401 (2015).
[12] G. Ritt, C. Geckeler, T. Salger, G. Cennini, and M. Weitz, Phys. Rev. A **74**, 063622 (2006).
[13] B. Brezger, T. Schulze, P. Schmidt, R. M. T. Pfau, and J. Mlynek, Europhys. Lett. **46**, 148 (1999).
[14] T. Salger, C. Geckeler, S. Kling, and M. Weitz, Phys. Rev. Lett. **99**, 190405 (2007).
[15] N. Lundblad, P. J. Lee, I. B. Spielman, B. L. Brown, W. D. Phillips, and J. V. Porto, Phys. Rev. Lett. **100**, 150401 (2008).
[16] M. Lukin, Rev. Mod. Phys. **75**, 457 (2003).
[17] N. V. Vitanov, A. A. Rangelov, B. W. Shore, and K. Bergmann, arXiv:1605.00224.
[18] S. Baier, M. Mark, D. Petter, K. Aikawa, L. Chomaz, Z. Cai, M. Baranov, P. Zoller, and F. Ferlaino, Science **352**, 201 (2016).
[19] N. Q. Burdick, Y. Tang, and B. L. Lev, Phys. Rev. X **6**, 031022 (2016).
[20] H. Kadau, M. Schmitt, M. Wenzel, C. Wink, T. Maier, I. Ferrier-Barbut, and T. Pfau, Nature (London) **530**, 194 (2016).
[21] I. Ferrier-Barbut, H. Kadau, M. Schmitt, M. Wenzel, and T. Pfau, Phys. Rev. Lett. **116**, 215301 (2016).
[22] A. de Paz, A. Sharma, A. Chotia, E. Maréchal, J. H. Huckans, P. Pedri, L. Santos, O. Gorceix, L. Vernac, and B. Laburthe-Tolra, Phys. Rev. Lett. **111**, 185305 (2013).
[23] C. Gardiner and P. Zoller, *The Quantum World of Ultra-Cold Atoms and Light Book II: The Physics of Quantum-Optical Devices* (World Scientific, Singapore, 2015), p. 1.
[24] A. V. Gorshkov, L. Jiang, M. Greiner, P. Zoller, and M. D. Lukin, Phys. Rev. Lett. **100**, 093005 (2008).
[25] This is in contrast to spin-orbit coupling schemes based on running wave laser configurations with Λ systems [63].
[26] A. P. Kazantsev, G. Surdutovich, and V. Yakovlev, *Mechanical Action of Light on Atoms* (World Scientific, Singapore, 1990).
[27] R. Dum and M. Olshanii, Phys. Rev. Lett. **76**, 1788 (1996).
[28] S. K. Dutta, B. K. Teo, and G. Raithel, Phys. Rev. Lett. **83**, 1934 (1999).
[29] J. Ruseckas, G. Juzeliūnas, P. Öhberg, and M. Fleischhauer, Phys. Rev. Lett. **95**, 010404 (2005).
[30] K. Bergmann, N. V. Vitanov, and B. W. Shore, J. Chem. Phys. **142**, 170901 (2015).
[31] E. Merzbacher, *Quantum Mechanics* (Wiley, New York, 1998).
[32] See Supplemental Material http://link.aps.org/supplemental/10.1103/PhysRevLett.117.233001 for extended discussions and details of analytical and numerical calculations, which includes [33–45].
[33] S. Yi and L. You, Phys. Rev. A **61**, 041604 (2000).
[34] S. Ronen, D. C. E. Bortolotti, D. Blume, and J. L. Bohn, Phys. Rev. A **74**, 033611 (2006).
[35] S. Sinha and L. Santos, Phys. Rev. Lett. **99**, 140406 (2007).
[36] F. Gerbier, A. Widera, S. Fölling, O. Mandel, T. Gericke, and I. Bloch, Phys. Rev. A **72**, 053606 (2005).
[37] I. Bloch, Nat. Phys. **1**, 23 (2005).
[38] T. Stöferle, H. Moritz, C. Schori, M. Köhl, and T. Esslinger, Phys. Rev. Lett. **92**, 130403 (2004).

[39] C. Kollath, A. Iucci, T. Giamarchi, W. Hofstetter, and U. Schollwöck, Phys. Rev. Lett. **97**, 050402 (2006).
[40] S. Gupta, Z. Hadzibabic, M. Zwierlein, C. Stan, K. Dieckmann, C. Schunck, E. Van Kempen, B. Verhaar, and W. Ketterle, Science **300**, 1723 (2003).
[41] Y. Shin, C. H. Schunck, A. Schirotzek, and W. Ketterle, Phys. Rev. Lett. **99**, 090403 (2007).
[42] P. Törmä and P. Zoller, Phys. Rev. Lett. **85**, 487 (2000).
[43] C. Chin, M. Bartenstein, A. Altmeyer, S. Riedl, S. Jochim, J. H. Denschlag, and R. Grimm, Science **305**, 1128 (2004).
[44] C. A. Regal, C. Ticknor, J. L. Bohn, and D. S. Jin, Nature (London) **424**, 47 (2003).
[45] M. Łącki, A. Elben, H. Pichler, M. A. Baranov, and P. Zoller (to be published).
[46] D.-W. Wang, M. D. Lukin, and E. Demler, Phys. Rev. Lett. **97**, 180413 (2006).
[47] A. Pikovski, M. Klawunn, G. V. Shlyapnikov, and L. Santos, Phys. Rev. Lett. **105**, 215302 (2010).
[48] M. A. Baranov, A. Micheli, S. Ronen, and P. Zoller, Phys. Rev. A **83**, 043602 (2011).
[49] M. A. Baranov, M. Dalmonte, G. Pupillo, and P. Zoller, Chem. Rev. **112**, 5012 (2012).
[50] $a_D = 21$ nm for Dy atoms, for polar molecules it is typically of the order of ~100 nm and higher.
[51] B. Yan, S. A. Moses, B. Gadway, J. P. Covey, K. R. Hazzard, A. M. Rey, D. S. Jin, and J. Ye, Nature (London) **501**, 521 (2013).
[52] S. A. Moses, J. P. Covey, M. T. Miecnikowski, B. Yan, B. Gadway, J. Ye, and D. S. Jin, Science **350**, 659 (2015).
[53] For transverse confinement $\ell_\perp$ with a nonresonant optical lattice we note the condition $\ell > \ell_\perp$.
[54] O. Mandel, M. Greiner, A. Widera, T. Rom, T. W. Hänsch, and I. Bloch, Phys. Rev. Lett. **91**, 010407 (2003).
[55] P. J. Lee, M. Anderlini, B. L. Brown, J. Sebby-Strabley, W. D. Phillips, and J. V. Porto, Phys. Rev. Lett. **99**, 020402 (2007).
[56] P. Soltan-Panahi, J. Struck, P. Hauke, A. Bick, W. Plenkers, G. Meineke, C. Becker, P. Windpassinger, M. Lewenstein, and K. Sengstock, Nat. Phys. **7**, 434 (2011).
[57] H.-N. Dai, B. Yang, A. Reingruber, X.-F. Xu, X. Jiang, Y.-A. Chen, Z.-S. Yuan, and J.-W. Pan, Nat. Phys. **12**, 783 (2016).
[58] Y. J. Lin, K. Jiménez-García, and I. B. Spielman, Nature (London) **471**, 83 (2011).
[59] P. Wang, Z.-Q. Yu, Z. Fu, J. Miao, L. Huang, S. Chai, H. Zhai, and J. Zhang, Phys. Rev. Lett. **109**, 095301 (2012).
[60] L. W. Cheuk, A. T. Sommer, Z. Hadzibabic, T. Yefsah, W. S. Bakr, and M. W. Zwierlein, Phys. Rev. Lett. **109**, 095302 (2012).
[61] B. K. Stuhl, H. I. Lu, L. M. Aycock, D. Genkina, and I. B. Spielman, Science **349**, 1514 (2015).
[62] L. Huang, Z. Meng, P. Wang, P. Peng, S.-L. Zhang, L. Chen, D. Li, Q. Zhou, and J. Zhang, Nat. Phys. **12**, 540 (2016).
[63] V. Galitski and I. B. Spielman, Nature (London) **494**, 49 (2013).
[64] J. Dalibard, F. Gerbier, G. Juzeliūnas, and P. Öhberg, Rev. Mod. Phys. **83**, 1523 (2011).
[65] N. Goldman, J. C. Budich, and P. Zoller, Nat. Phys. **12**, 639 (2016).
[66] X. Cui, B. Lian, T.-L. Ho, B. L. Lev, and H. Zhai, Phys. Rev. A **88**, 011601 (2013).
[67] M. Mancini, G. Pagano, G. Cappellini, L. Livi, M. Rider, J. Catani, C. Sias, P. Zoller, M. Inguscio, M. Dalmonte, and L. Fallani, Science **349**, 1510 (2015).
[68] S. Nascimbène, J. Phys. B **46**, 134005 (2013).
[69] M. L. Wall, A. P. Koller, S. Li, X. Zhang, N. R. Cooper, J. Ye, and A. M. Rey, Phys. Rev. Lett. **116**, 035301 (2016).
[70] This requirement will be easier to satisfy with electric dipole moments from polar molecules than with magnetic atoms.
[71] A. Micheli, Z. Idziaszek, G. Pupillo, M. A. Baranov, P. Zoller, and P. S. Julienne, Phys. Rev. Lett. **105**, 073202 (2010).
[72] F. Jendrzejewski *et al.*, arXiv:1609.01285 [Phys. Rev. Lett. (to be published)].